

## MICRO-PARTICLE IMAGE VELOCIMETRY FOR IMAGING FLOWS IN PASSIVE MICROFLUIDIC MIXERS

Dariusz Witkowski<sup>1</sup>, Wojciech Kubicki<sup>2</sup>, Jan A. Dziuban<sup>2</sup>, Darina Jašíková<sup>3</sup>,  
Anna Karczemka<sup>1</sup>

- 1) Lodz University of Technology, Institute of Turbomachinery, Wólczańska 219/223, 90-924 Łódź, Poland  
(✉ [dariusz.witkowski@p.lodz.pl](mailto:dariusz.witkowski@p.lodz.pl), 48 42 631 2452, [anna.karczemka@p.lodz.pl](mailto:anna.karczemka@p.lodz.pl))
- 2) Wrocław University of Science and Technology, Division of Microengineering and Fotovoltaics,  
Długa 61, 53-633 Wrocław, Poland ([wojciech.kubicki@pwr.edu.pl](mailto:wojciech.kubicki@pwr.edu.pl), [jan.dziuban@pwr.edu.pl](mailto:jan.dziuban@pwr.edu.pl))
- 3) Technical University of Liberec, Institute of Novel Technologies and Applied Informatics,  
Studentska 1402/2, 461 17 Liberec 1, Czech Republic ([darina.jasikova@tul.cz](mailto:darina.jasikova@tul.cz))

### Abstract

The micro-Particle Image Velocimetry (micro-PIV) was used to measure flow velocities in micro-channels in two passive micromixers: a microfluidic Venturi mixer and a microfluidic spiral mixer, both preceded by standard “Y” micromixers. The micro-devices were made of borosilicate glass, with micro-engineering techniques dedicated to micro-PIV measurements. The obtained velocity profiles show differences in the flow structure in both cases. The micro-PIV enables understanding the micro-flow phenomena and can help to increase reproducibility of micromixers in mass production.

Keywords: micro-Particle Image Velocimetry, microfluidics, microfluidic devices.

© 2018 Polish Academy of Sciences. All rights reserved

## 1. Introduction

In the second half of the twentieth century a rapid development in the field of miniaturization, especially evident in electronics, took place. Advances in micro-technology and biological sciences (including discovery of the DNA structure in 1953, development in techniques related to the analysis of DNA and proteins *etc.*) led to extensive interest in those areas in the early 1990s. Many ideas of miniaturization of conventional techniques for the analysis of biomolecules and production of micro-devices, like lab-on-a-chip and  $\mu$ TAS (micro-Total Analysis System) microfluidic devices, were developed [1–9, 19–21]. Micro-devices are mainly built of silicon, glass or polymers and they employ, depending on their application, a network of specially designed micro-channels, microelectrodes, micro-valves, or microelectronic devices and transducers, such as biosensors, *etc.* They are used in various processes such as, for instance, electrophoretic separation (electrophoresis chips), chromatography, specific amplification of DNA fragments by the *polymerase chain reaction* (PCR). They can also be applied in different stages of chemical reactions, mixing fluids, *etc.*

In the opinion of many scientists, microfluidic devices will change the world and our laboratories in the twenty-first century like microelectronics altered the world in the twentieth century.

For over 20 years microfluidic investigations have developed dynamically. However, still many issues remain unsolved in this field. In addition, further miniaturization leads to nano-flows, where the known phenomena and laws from fluid mechanics completely collapse.

Therefore, a growing interest in understanding flowing phenomena at the microscale and, recently, nanoscale level, can be observed as well. There is also a need to perform accurate flow measurements. The micro-Particle Image Velocimetry is a technique for measuring velocity fields at the microscopic level. This method was miniaturized to measure the velocities of micro-flows to diagnose microfluidic devices. The first micro-PIV measurement was performed by Santiago, Wereley, Meinhart in 1998 and 1999 [10, 11].

Issues associated with micro-mixing of liquids and metrology of micro-flows and microfluidic devices are extremely interesting from the scientific point of view.

The future large scale production of microfluidic devices for many different applications needs to identify and develop metrological techniques for their characterization [12, 13]. A general set of aspects critical for microfluidic devices include three main categories, namely: dimensions and geometry (microchannel widths, heights), surface properties (roughness, flatness) and sub-surface properties (defects or bubbles at interfaces *etc.*). Shilpiekandula in [12] shows different metrological techniques, such as atomic force microscopy, interferometry and confocal microscopy, for the high throughput production of polymer-based microfluidic devices. Many metrological tools are similar as in the area of semiconductor and *microelectromechanical system* (MEMS) manufacturing. The micro-PIV technique was also applied to characterize microchannel geometry parameters by Silva [14].

The problem of mixing liquids in microscale turns out to be much more complex than at the macro level [15–16]. The fluid flow in micro-channels is laminar. The mixing of a liquid is here influenced by the diffusion phenomenon, due to the absence of turbulence. In the past two decades all sorts of micromixers were developed, often on the basis of empirical designs only. These devices can be divided into two groups: passive and active micromixers. Passive micromixers have an appropriate geometry of micro-channels/microstructures that enables to increase the contact area between liquid streams. For example, micro-channels introduced into the microstructure disrupt the flow nature, thus changing the flow rate and direction of each plane. There are many different designs of such micromixers. Active micromixers use an additional external force which introduces turbulence into the micro-flow. Many techniques are applied to achieve this effect, *e.g.* ultrasonic generation, temperature gradients, electric or magnetic fields, pulsed injection of the liquid, *etc.* In this paper, we focus on imaging flows in two passive mixers.

The *Particle Image Velocimetry* (PIV) measures whole velocity fields by taking two images shortly one after another and calculating the distance individual particles travelled within this time [17–18]. From the known time difference and the measured displacement, the velocity is calculated. Since the flow can be quite fast, one has to avoid blurred images and that is one reason why laser pulses, which last for 6–10 ns only and enable recording of frozen motion, are used. Another reason is that only laser light can be focused into a thin enough light sheet so that only particles in that plane are imaged. Otherwise the scattered light from particles in other planes would make this measurement impossible. A special camera is used to store the first image (frame) fast enough to be ready for the second exposure. The “dead” time between the frames when the camera is “blind” is as short as 100 ns.

The PIV system can be used for measuring velocities in a variety of devices such as liquid and gas flow investigations in wind tunnels, water channels, in-cylinder engines, industrial flow systems, compressors, turbines, fans, pumps, *Micro Electro Mechanical Systems* (MEMS).

Micro-PIV systems are designed to measure flow fields in microscale by employing dedicated microscopic imaging components. In the micro-PIV, the light sheet applied in planar PIV

applications is replaced by the volume illumination of the flow, and the depth of field is determined by the numerical aperture of the microscope objective lens. Fluorescent particles are used for flow seeding to remove the strong background light from the nearby surfaces. The fluorescent light is red-shifted from the excitation light and separated with a filter cube. An additional feature of the micro-flow is a low Reynolds number (no turbulent effect) and an influence of the Brownian motion. The double frame images are evaluated with conventional PIV algorithms.

The aim of this paper is to show the micro-PIV technique applied to velocity measurements in two microfluidic mixers of different geometries and to discuss applicability of the micro-PIV to metrology of microfluidic devices. The element of novelty is an entirely glass-made, original design, dedicated to micro-PIV measurements, without layers of glue or polymers, which provides constant physicochemical properties in micro-channels.

## 2. Microfluidic mixers

Micro-PIV measurements were performed with two solutions of passive microfluidic mixers: firstly, a spiral-shaped microchannel and, secondly, Venturi-type tubes in a straight microchannel, both preceded by standard Y-mixers. The micro-devices were made entirely of glass, by means of dedicated micro-engineering techniques.

Glass as a material used for chips shows a number of advantages, especially in comparison with more popular solutions, technologically easier, cheaper and generally available, *i.e.* polymer chips:

- it is chemically resistant, so it does not introduce any impurities into a liquid sample and does not adsorb anything from the solution, thus it ensures the repeatability of process conditions;
- it is optically transparent, thus flow observation and fluorescence excitation of particles in the solution are possible;
- it allows chips to be used many times and, therefore, the process can be repeated in the same conditions, which is usually difficult or impossible for the majority of other chips;
- it is not deformed under influence of pressure and/or temperature and/or time, like most polymers, so the flow conditions are reproducible;
- the auto-fluorescence of glass is much lower than the auto-fluorescence of most of polymers, so it is better suited to the micro-PIV method.

All these aspects enable to enter new areas of research.

A spiral micromixer (Fig. 1) is built of a spiral main channel with 16 serpents, each providing a  $180^\circ$  change in the fluid flow direction. Fluids A and B are supplied by two dosing channels, set at an angle of  $90^\circ$ , into the preliminary mixing area of the Y-crossing. Next, the fluids are mixed in the spiral mixer of the total length of 86 mm. All micro-channels are isotropically etched, and

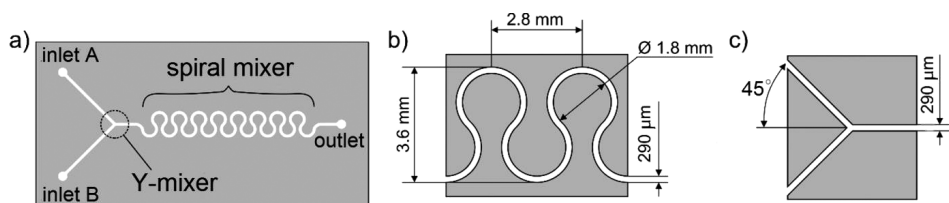


Fig. 1. A scheme of a microfluidic spiral mixer – fluids are preliminary mixed in the Y-type crossing and next in the main channel with 16 serpents: a layout of micro-channels (a); magnified views of a serpent (b); the Y-mixer (c).

their nominal widths are  $290\ \mu\text{m}$  at the top and  $190\ \mu\text{m}$  at the bottom, the total depth is equal to  $45\ \mu\text{m}$ , and the channel cross-section has the shape of an isosceles trapezium.

In the case of the second solution of the micromixer, fluids are initially mixed in the Y-crossing with a single Venturi tube (1 in Fig. 2) and next in two other double Venturi tubes (2 and 3 in Fig. 2) located along the 32-mm main straight channel. The width of all the channels is  $290\ \mu\text{m}$  at the top, except Venturi tubes, where the channel is narrowed to  $190\ \mu\text{m}$ . To enable better observation of the preliminary mixing, the first Venturi tube was elongated to  $800\ \mu\text{m}$ , whereas the other two were  $500\ \mu\text{m}$  long.

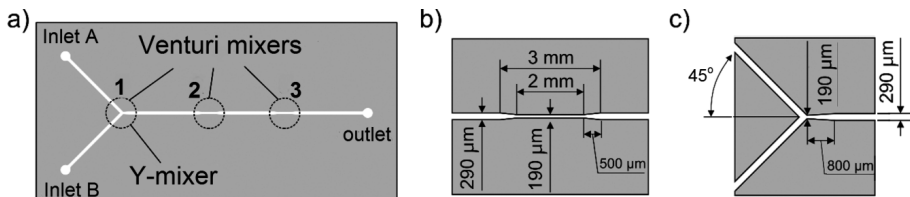


Fig. 2. A scheme of a microfluidic Venturi mixer – fluids are preliminary mixed in the Y-mixer with a single Venturi tube (1) and next in two double Venturi tubes in the main channel (2 and 3); a layout of micro-channels (a); magnified views of a Venturi tube in the main channel (b); the Y-mixer with a single Venturi tube (c).

Each micro-device was made of two borosilicate glass substrates (Borofloat®33, Schott),  $50 \times 25 \times 1.1\ \text{mm}$  each (Fig. 3). Micro-channels were wet etched to the depth of  $45\ \mu\text{m}$  in the bottom substrate in 50% HF: 35% HCl (10:1) solution by means of a  $50\ \mu\text{m}$  thick masking layer of the positive photoresist (AZ40XT, Micro-chemicals) acting as an etch mask. The masking layer was patterned in a standard process of photolithography, and after etching it was removed in acetone. Via holes were mechanically drilled in the top substrate with a precise mill-drill system (BFW 40/E, Proxxon). Next, the top and bottom substrates were cleaned and permanently sealed in the fusion thermal bonding process at  $650^\circ\text{C}$ . Afterwards, PEEK microfluidic connectors (NanoPort N-333, IDEX) were sealed to the top surface of each micro-device, providing easy and tight connection of  $1/16''$  PTFE tubes with inlets and outlets.

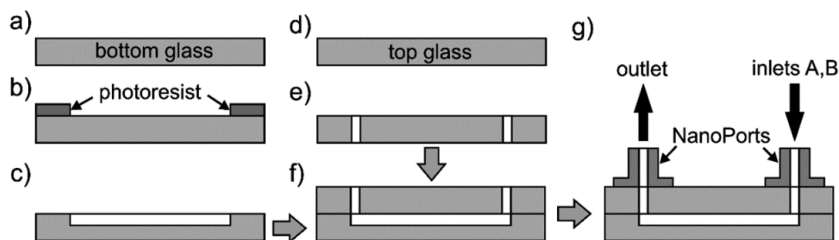


Fig. 3. A scheme of all-glass micromixer technology; the bottom glass substrate: cleaning (a); patterning etch mask of the photoresist (b); wet etching of micro-channels and mask removal (c); the top glass substrate: cleaning (d); drilling of vias (e); thermal fusion bonding of glass structures (f); adhesive bonding of standard microfluidic connectors (g).

### 3. Measurement test stand

The test stand (Fig. 4a) consisted of a New Wave Gemini Nd:YAG pulsed laser with a wavelength of  $532\ \text{nm}$  and the maximum energy of  $120\ \text{mJ}$  in each pulse. The laser light beam was directed towards a microfluidic device (passageway) through a dichroic filter. This filter selectively

passes the dichroic spectrum in a range of wavelengths, which is the main difference between the PIV and the micro-PIV. The laser light illuminates the volume of the channel in which there is a fluid with particles of inoculation. The fluid flow is forced by two syringe pumps pushing the liquid into the micromixer channel. A detection system comprises a CMOS camera placed above the chip and a computer with an appropriate software enabling capturing, processing and storing consecutive images.

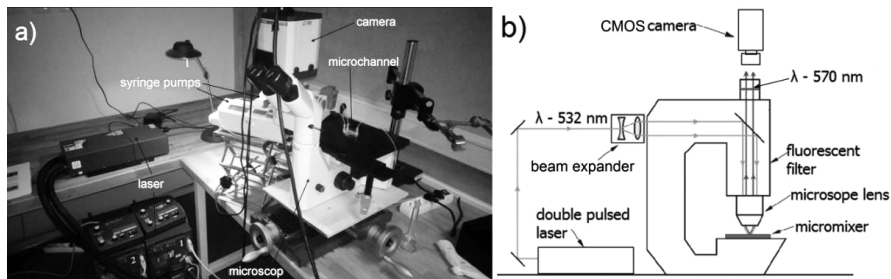


Fig. 4. The experimental test stand: a photo (a); a scheme (b).

Syringe pumps forcing the liquid flow into microchips and a Leica DM IL inverted laboratory microscope set with a standard objective (10× magnification for optimal imaging of microchannels) were used during the measurements. A Neo CMOS camera with 5.5 MPixel resolution and 6.5 μm pixel size recorded the movement of particles (Fig. 4b). At the beginning of the measurement, fluorescent particles (Rhodamine B particles that emit light with a wavelength of 570 nm) of a diameter equal to 1 μm were subject to test. Due to insufficient light emission, seeding particles were changed to those of a bigger diameter equal to 2 μm. A laser light beam through an optical fibre reaches the measuring channel in which 2 μm diameter particles containing Rhodamine B are placed. Rhodamine B absorbs laser radiation of a wavelength of 532 nm and emits fluorescence radiation of a wavelength of approx. 570 nm. The latter radiation is passed through a dichroic filter and travels to the CMOS camera.

Dantec Dynamics software – DynamicStudio was used in the measurements, whereas the results were analysed with Lavisision software – DaVis 8.2. An initial interrogation region size was 64 × 64 pixels, with a final size of 32 × 32 pixels and a 75% overlap region. The average particle displacement within an interrogation window is determined by a cross-correlation followed by the location of the correlation peak. A subtract sliding filter with a scale length of 3 pixels was employed in the image pre-processing. For the vector post-processing a median filter (“strongly remove and iteratively replace”) removing groups with fewer than 5 vectors, and smoothing (1 × smooth 3 × 3) were applied. The final vector resolution was equal to 58 vectors/mm.

The microchip was mounted on the transparent platform of the detector, which had been placed underneath. Three Teflon tubes were used: two coming from the syringe pumps to provide the fluid flow between the micro-device and the pumps, and the third one leading to the waste container.

Measurements were made for three different combinations of the flow rates:  $1.389 \times 10^{-9} \text{ m}^3/\text{s}$ ,  $2.778 \times 10^{-9} \text{ m}^3/\text{s}$ , and  $4.167 \times 10^{-9} \text{ m}^3/\text{s}$  (Table 1).

The microchannel (Fig. 5a) was divided into measurement areas, due to limited capabilities of the lens. The inlets are labelled as inlet A and inlet B. The measurement line is located at a distance of 460 μm from the point O (Fig. 5b), behind the connection of inlet A and inlet B.

Table 1. Measurement combinations of the flow rates.

inlet	flow rate [m <sup>3</sup> /s]	abbreviation
A	$1.389 \times 10^{-9}$	A1
A	$2.778 \times 10^{-9}$	A2
A	$4.167 \times 10^{-9}$	A3
B	$1.389 \times 10^{-9}$	B1
B	$2.778 \times 10^{-9}$	B2
B	$4.167 \times 10^{-9}$	B3

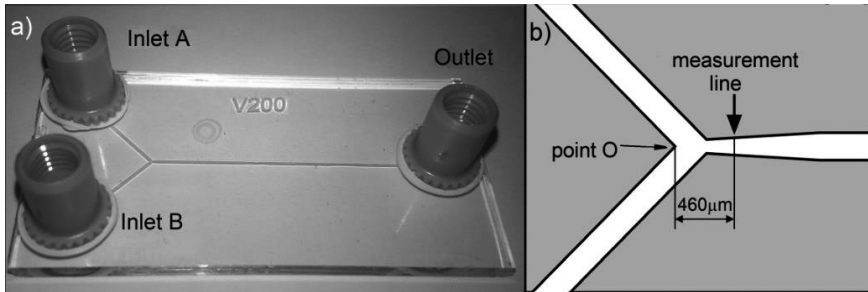


Fig. 5. A glass micromixer with Venturi tubes: a view of a chip (a); a layout of the micro-PIV measurement line (b).

#### 4. Results

In Fig. 6, a photo taken during the measurements is presented, where the size of particles in the channel is equal to  $2 \mu\text{m}$ . In Fig. 7a, the results of the flow rate at inlet A1 and inlet B3 are shown. Fig. 7b presents the results of the flow rate at the inlet to channel A3 and channel B3. The red arrow indicates the fluid flow direction.

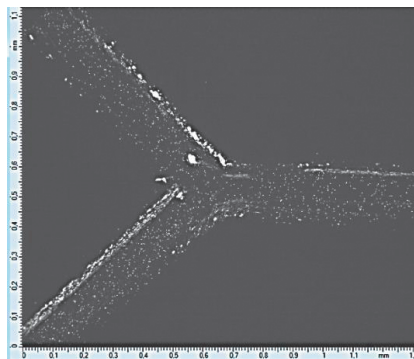


Fig. 6. A raw PIV image of the flow in the Venturi micromixer.

In Fig. 8, velocity distributions for different combinations of inlets A and B, along the measurement line, across the channel in the Y-mixer, are shown. It can be seen that the lower maximum velocity is obtained for lower values of inlet velocities, such as A1 and B1. Different values

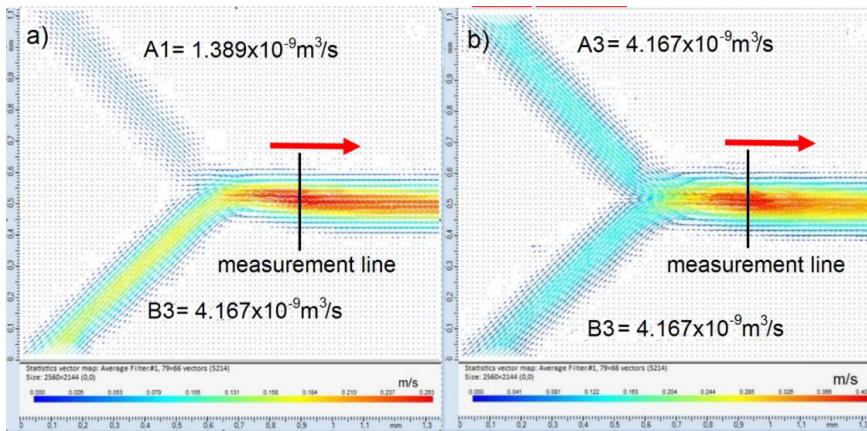


Fig. 7. Experimental results of velocity distributions for the channel of the Venturi micromixer in the Y-mixing area for flow rates A1 and B3, connection of inlets A and B (a); flow rates A3 and B3, connection of inlets A and B (b).

in the maximum speed for A1B2 and A2B1 are attained. The highest velocity value was achieved for A3B3 – approx. 0.42 m/s. For A1B2, the flow rate is 0.21 m/s, which represents 50% of the flow A3B3, which proves the measurement correctness. Despite the changes in the value of the flow rate in channel inlets A and B, a symmetry in the main channel is visible. For different flow values of channels A and B, e.g. A2B3, A1B3, A1B2, the curve is shifted to the left or right side of the plot.

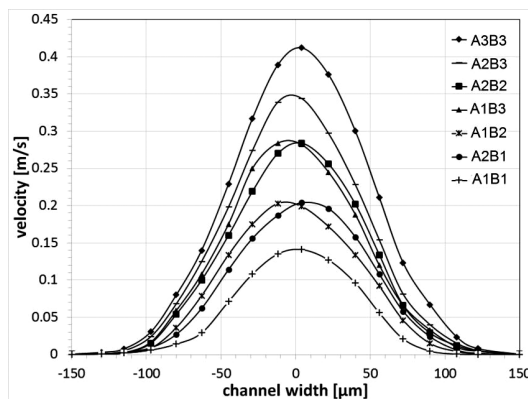


Fig. 8. A plot of velocity distributions along the measurement line, connection of inlets A and B.

Figure 9a shows a part of the Venturi micromixer during the measurement, say, a Venturi tube. A velocity distribution is presented in Fig. 9b. One can see that the velocity is higher in the contraction (0.378 m/s) than in the inlet of the Venturi tube (0.26 m/s).

The maximum velocity for the case of A1B1 is 0.16 m/s and it is three times lower than for the maximal flow in the case of A3B3 (0.475 m/s) (Fig. 10). For the flows A2B3 and A1B3, an

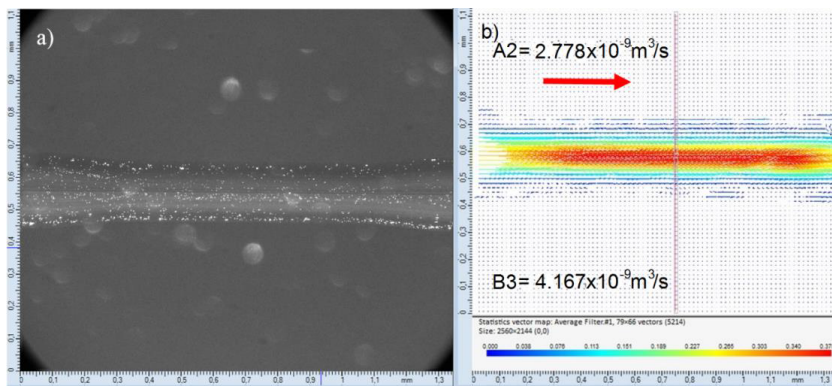


Fig. 9. The Venturi micromixer microchip a raw PIV image from the measurement, a Venturi tube (a); experimental results of the velocity distribution for the channel of the Venturi micromixer microchip for the flow rates A2 and B3, a Venturi tube (b).

asymmetrical flow is visible. The curve is shifted to the left, where the flow is less intensive, *i.e.* at inlet A.

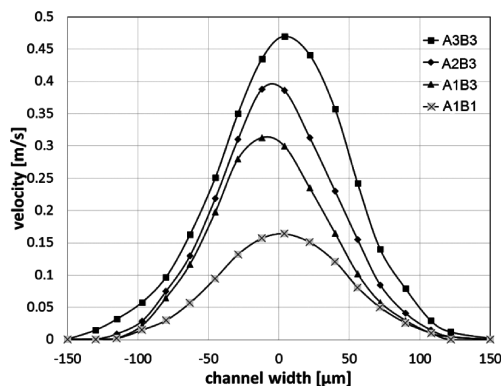


Fig. 10. A plot of velocity distributions along the measurement line, a Venturi tube.

Figure 11 shows measurement lines in successive loops in the channel serpent micromixer. The velocity was studied in six consecutive loop channels referred to from 1up to 6up. A plot of velocity distributions along the lines is drawn in Fig. 12.

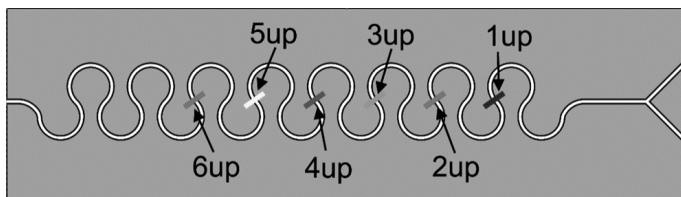


Fig. 11. A scheme of a serpent micromixer microchannel with marked micro-PIV measurement areas in consecutive serpents.



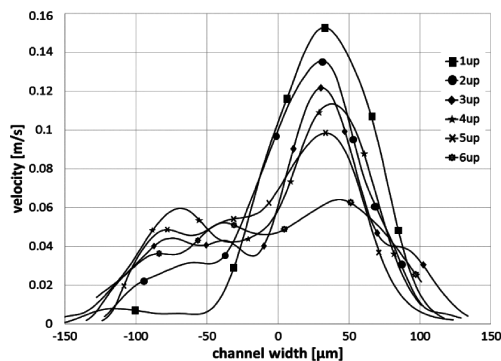


Fig. 12. A plot of velocity distributions along the measurement lines, a serpent micromixer microchannel.

As can be seen, as it moves away from the inlet channels, the maximum flow rate begins to decrease. For the first loop (1up), the maximum velocity is equal to 0.153 m/s, whereas for the last loop (6up), the peak velocity equals 0.064 m/s. A lack of symmetry is seen for each of the flows, higher velocities being recorded in the inner part of the channel. The difference in the maximum velocity between the first and second serpentine is approx. 11%, further differences between serpentines are on a similar level. The only exception is the difference between serpentines 5up and 6up, equal to about 34%. The maximum velocity value is decreasing, but as the flow rate has to be the same, the velocity distribution is becoming wider. For example, in serpentine 1up, the flow is between  $-50 \mu\text{m}$  and  $115 \mu\text{m}$ , whereas in serpentine 5up the flow is between  $-150 \mu\text{m}$  and  $120 \mu\text{m}$ , which is about 60% greater.

## 5. Conclusions

In the recent years accurate measurements and control of liquid micro-flows have become more and more important for numerous applications, hence metrology of micro-flows and metrology of microfluidic devices have gained an increasing importance. The micro-PIV technique has been demonstrated to measure velocity fields in two passive micromixers made of glass. The original borosilicate glass has been manufactured with techniques dedicated to micro-PIV engineering, without layers of glue or polymers. A microfluidic Venturi mixer and a microfluidic spiral mixer have been examined. At the same inlet velocities, the results show some differences in velocity distributions. The glass microfluidic devices exhibit many advantages over the PDMS ones. Glass is optically transparent, has low auto-fluorescence for the laser used, is chemically resistant and, therefore, easy to clean, has a rigid and non-deformable design compared with the PDMS chips. In general, the micro-PIV enables characterization of microfluidic devices, thus in the future it can help increase reproducibility of micromixers and other microfluidic devices during their mass production.

## References

- [1] Whitesides, G.M. (2006). The origin and the future of microfluidics. *Nature*, 442/27, 368–373.
- [2] Manz, Harrison, D., Verpoorte, E., Fettingner, J., Paulus, A., Ludi, H., Widmer, H.J. (1992). *Chromatogr*, A593, 253.

- [3] Bargiel, S., Górecka-Drzazga, A., Dziuban, J., Prokaryn, P., Chudy, M., Dybko, A., Brzózka, Z. (2004). Nanoliter detectors for flow systems. *Sensors and Actuators. A, Physical.*, 115(2/3), 245–251.
- [4] Kubicki, W., Walczak, R., Dziuban, J. (2011). Injection, separation and fluorimetric detection of DNA in glass lab-on-a-chip for capillary gel electrophoresis. *Optica Applicata.*, 41(2), 409–416.
- [5] Śniadek, P., Walczak, R., Dziuban, J., Jackowska, M., Antosik, P., Jaśkowski, J., Kempisty, B. (2011). Lab-on-a-chip for quality classification of pig oocytes. *Optica Applicata.*, 41(2), 417–422.
- [6] Bembnowicz, P., Małodobra, M., Kubicki, W., Śniadek, P., Górecka-Drzazga, A., Dziuban, J., Jonkisz, A., Karpiewska, A., Dobosz, T., Golonka, L. (2010). Preliminary studies on LTCC based PCR microreactor. *Sensors and Actuators. B, Chemical.*, 150(2), 715–721.
- [7] Karczemska, A., Ralchenko, V., Bolshakov, A., Sovyk, D., Łysko, J.M., Fijałkowski, M., Hassard, J. (2011). Application of Diamond for Microfluidic Devices in. *Implantexpert*, ed. Nawrat, Z., Zabrze, 107–116.
- [8] Karczemska, A. (2013). Diamond materials for microfluidic devices, in diamond-based materials for biomedical applications. ed. Narayan, R., *Woodhead Publishing Series in Biomaterials.*, 55, Woodhead Publishing Limited, 256–271.
- [9] Karczemska, A.T., Witkowski, D., Ralchenko, V., Bolshakov, A., Sovyk, D., Łysko, J.M., Fijałkowski, M., Bodzenta, J., Hassard, J. (2011). Diamond electrophoretic microchips – Joule heating effects. *Materials Science and Engineering B*, 176, 326–330.
- [10] Santiago, J.G., Wereley, S.T., Meinhart, C.D., Beebe, D.J., Adrian, R.J. (1998). A particle image velocimetry system for microfluidics. *Experiments in Fluids*, 25, 316–319.
- [11] Meinhart, C.D., Wereley, S.T., Santiago, J.G. (1999). PIV measurements of a microchannel flow. *Experiments in Fluids*, 27, 414–419.
- [12] Shilpiekandula, V., Burns, D.J., Rifai, K.E., Youcef-Toumi, K., Shiguang, L. (2006). I Reading and S Fatt Yoon. *Metrology of Microfluidic Devices: A Review*, ICOMM, 49.
- [13] Karczemska, A., Witkowski, D. (2012). Metrology of microfluidic devices. *Ciepłne Maszyny Przepływowe – Turbomachinery*, 142, 55–73.
- [14] Silva, G., Leal, N., Semiao, V. (2009). Determination of microchannels geometric parameters using micro-PIV. *Chemical Engineering Research and Design*, 87, 298–306.
- [15] Gambhire, S., Patel, N., Gambhire, G., Kale, S. (2016). A Review on Different Micromixers and its Micromixing within Microchannel. *International Journal of Current Engineering and Technology*, 4.
- [16] Lee, Ch-Y., Chang, Ch-L., Wang, Y-N., Fu, L-M. (2011). Microfluidic Mixing: A Review. *Int. J. Mol. Sci.*, 12, 3263–3287.
- [17] Lai, W.T., Menon, R.K. (2004). Flow Measurements in Microchannels Using a MicroPIV system. *15th Australasian Fluid Mechanics Conference*, Sydney, Australia, 13–17.
- [18] Williams, S.J., Park, Ch., Wereley, S.T. (2010). Advances and applications on microfluidic velocimetry techniques – review. *Microfluid Nanofluid*, 8, 709–726.
- [19] Adamski, K., Kubicki, W., Walczak, R. (2016). 3D Printed electrophoretic lab-on-chip for DNA separation. *Procedia Engineering*, 168, 1454–1457.
- [20] Kubicki, W., Pająk, B., Kucharczyk, K., Walczak, R., Dziuban, J.A. (2016). Rapid detection of highly pathogenic A (H7N7) avian influenza virus genetic markers in heterogenic samples utilizing on-chip SSCP-CE method. *Sensors and Actuators B*, 236, 926–936.
- [21] Dziuban, J.A., Mróz, J., Szczygielska, M., Małachowski, M., Górecka-Drzazga, A., Walczak, R., Buła, W., Zalewski, D., Nieradko, Ł., Łysko, J., Koszur, J., Kowalski, P. (2004). Portable gas chromatograph with integrated components. *Sensors and Actuators A*, 115, 318–330.